Supporting Information

Mechanochemical Synthesis of Environmentally Benign Fully Biobased 4th Generation Benzoxazines and their Polymers: Mechanistic Insights Into Latent Catalyst Effect

Vaishaly Duhan,[1] Shivani Yadav,[1] Christophe Len[2,3] and Bimlesh Lochab[1]*

[1]Materials Chemistry Laboratory, Department of Chemistry, School of Natural Sciences, Shiv Nadar Institution of Eminence, Gautam Buddha Nagar, Uttar Pradesh 201314, India.

[2]School of Chemistry, Xi'an Jiaotong University, 28 Xianning West Road, Xi'an (China)

[3]Institute of Chemistry for Life and Health Sciences, Chimie ParisTech, PSL Research University, 11 rue Pierre et Marie Curie, Paris (France)

TOTAL: 16 Pages, 3 Table and 16 Figures

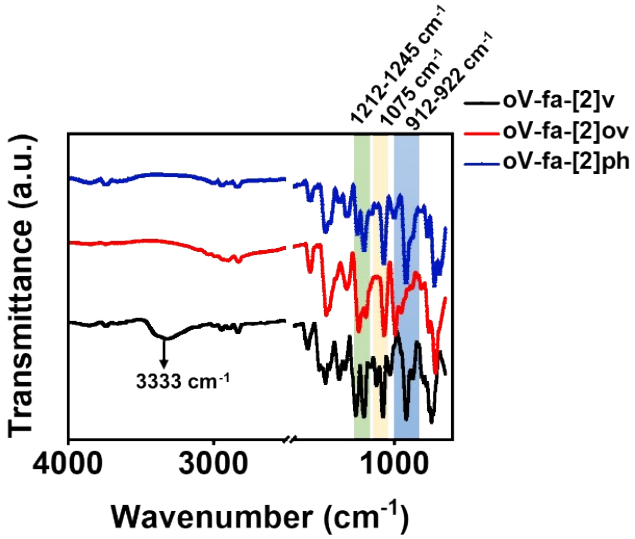

Fig. S1 FTIR spectra of monomers.

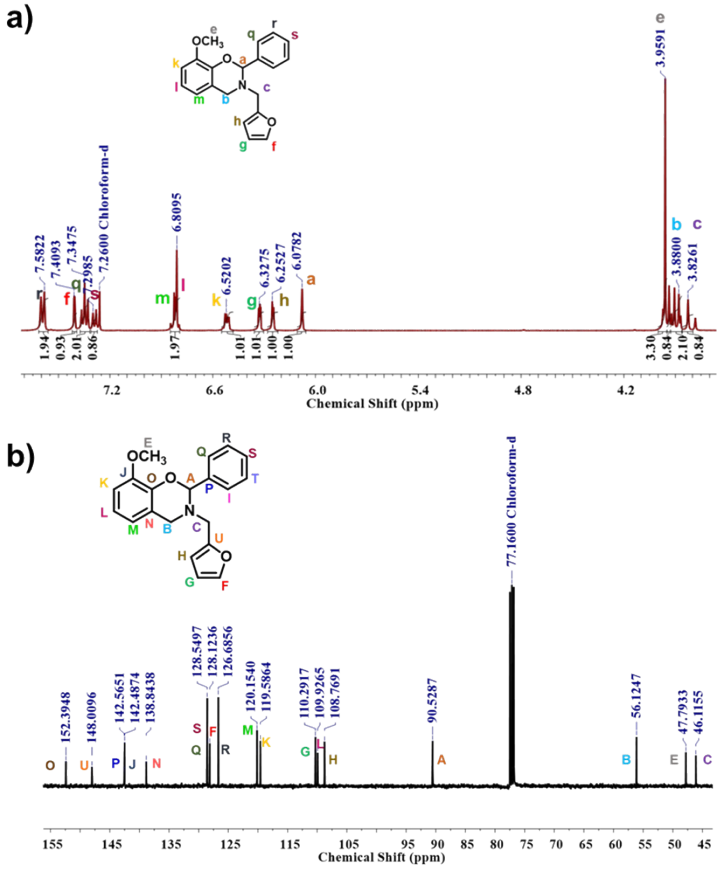

Fig. S2 NMR spectra of oV-*fa*-[2]ph monomer: (a) ^{1}H and (b) ^{13}C NMR.

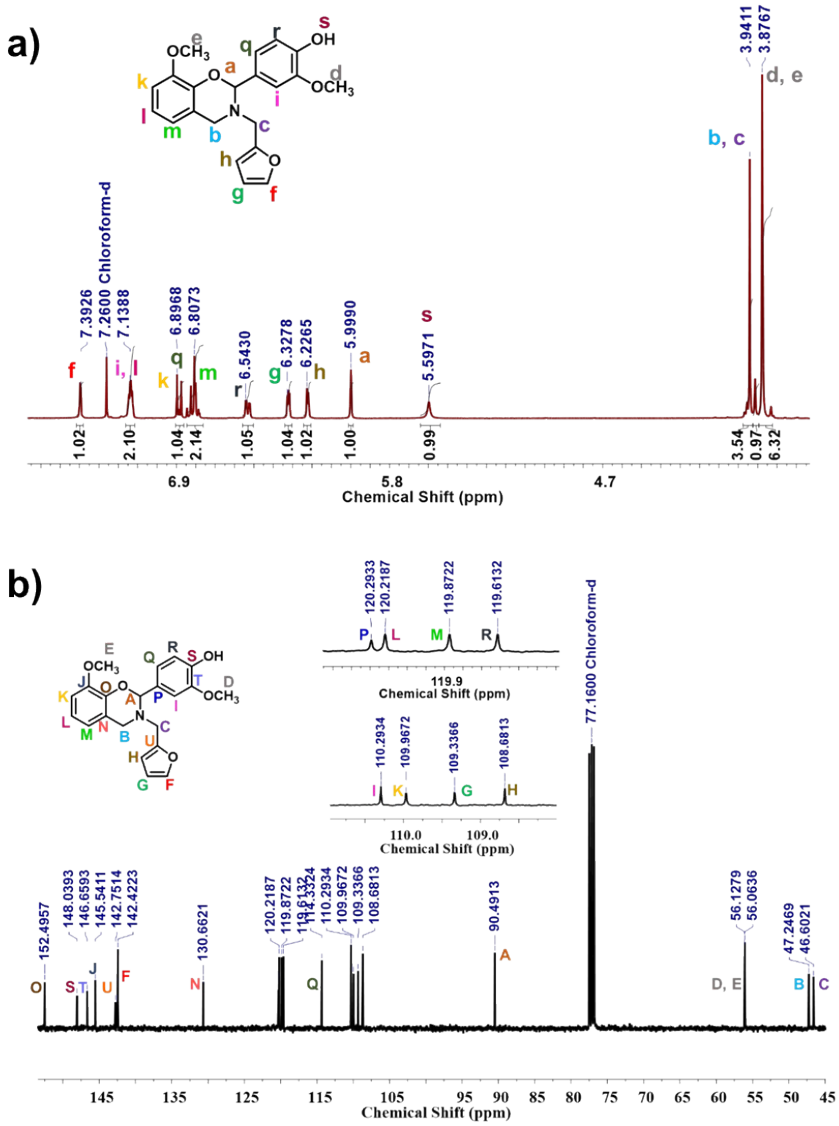

Fig. S3 NMR spectra of oV-*fa*-[2]v monomer: (a) ^{1}H and (b) ^{13}C.

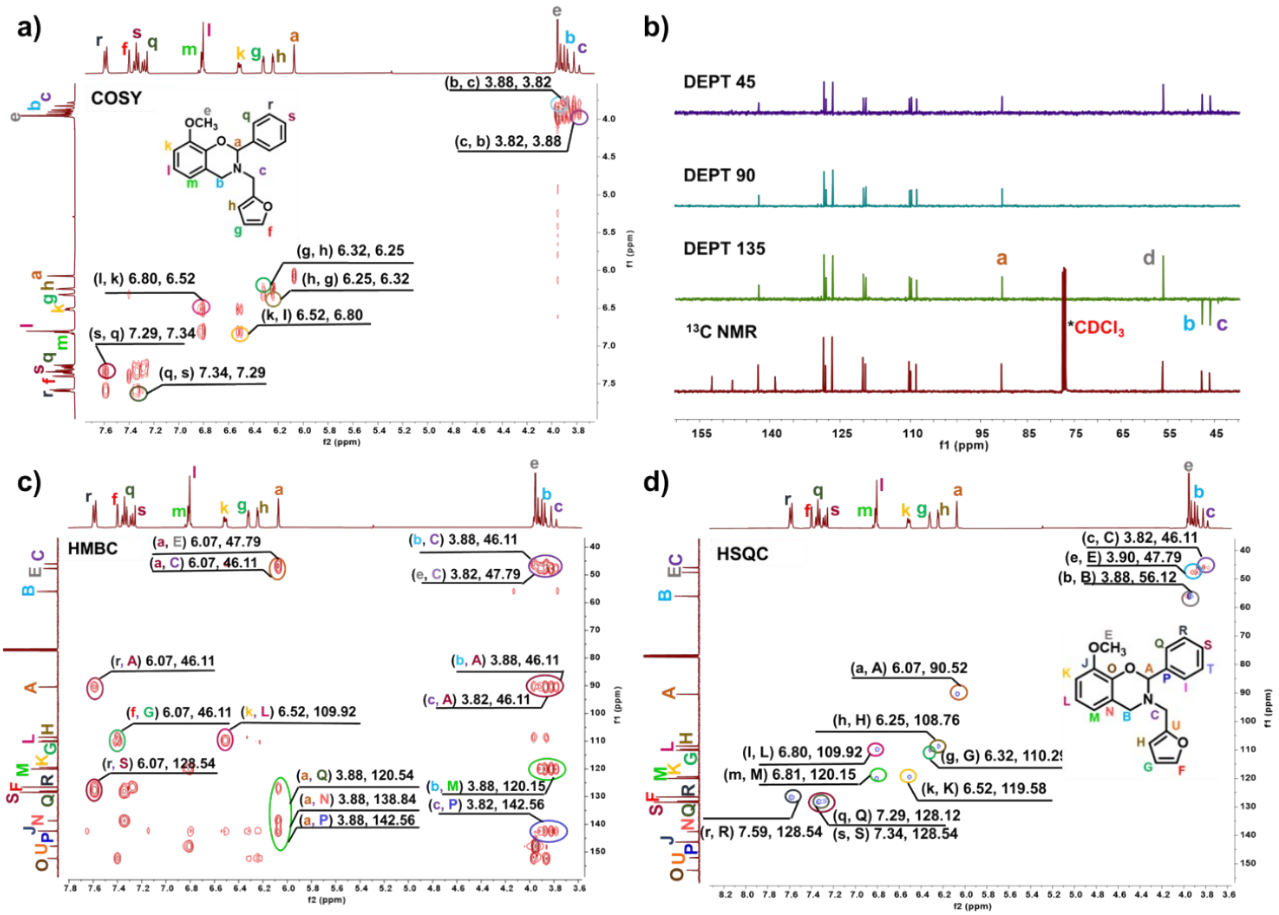

Fig. S4 NMR spectra of oV-*fa*-[2]ph: (a) 2D ^{1}H–^{1}H COSY; (b) Stacked ^{13}C and DEPT 45/90/135; (c) 2D ^{1}H–^{13}C HMBC; (d) 2D ^{1}H–^{13}C HSQC.

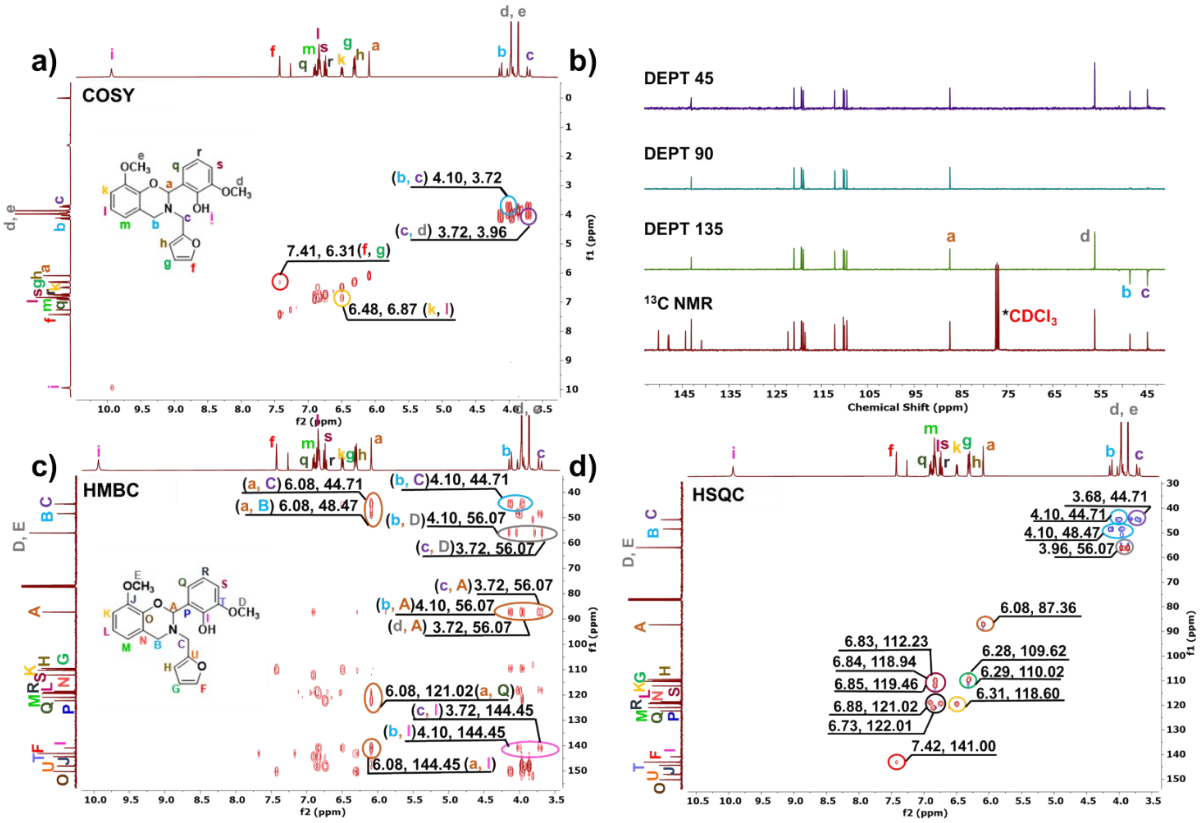

Fig. S5 NMR spectra of oV-*fa*-[2]ov: (a) 2D ^{1}H–^{1}H COSY; (b) Stacked ^{13}C and DEPT 45/90/135; (c) 2D ^{1}H–^{13}C HMBC; (d) 2D ^{1}H–^{13}C HSQC.

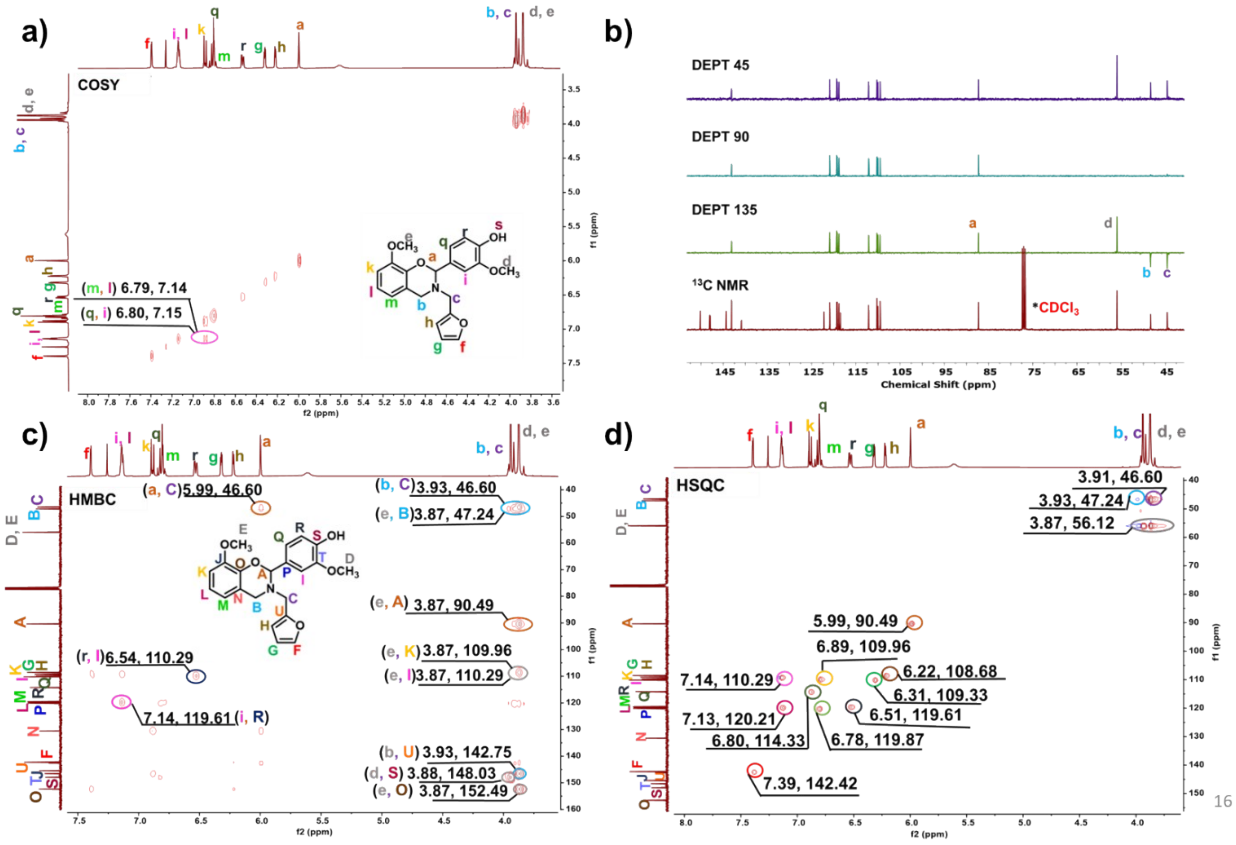

Fig. S6 NMR spectra of oV-fa-[2]v: (a) 2D ^{1}H–^{1}H COSY; (b) Stacked ^{13}C and DEPT 45/90/135; (c) 2D ^{1}H–^{13}C HMBC; (d) 2D ^{1}H–^{13}C HSQC.

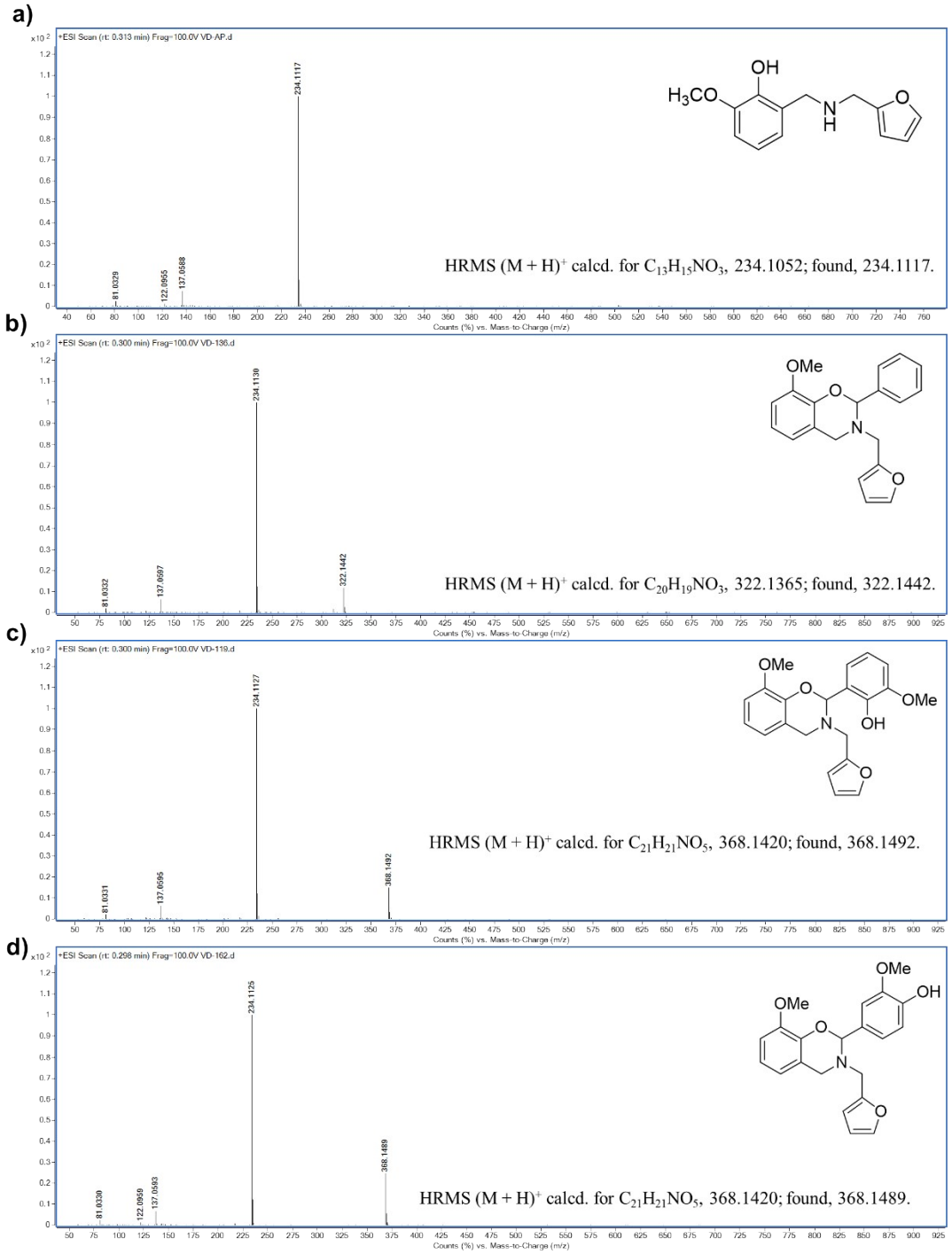

Fig. S7 HRMS spectra of monomers.

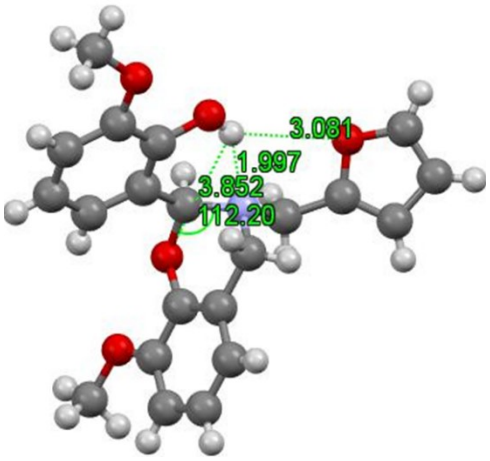

Fig. S8 ORTEP diagram of oV-*fa*-[2]ov at 40 °C.

Table S1 Crystal data for compound oV-*fa*-[2]ov. (CCDC: 2291158 (16 ºC), 2291159 (40 ºC) and 2291694 (70 ºC) contain the supplementary crystallographic data for this paper. These data can be obtained free of charge from The Cambridge Crystallographic Data Centre (CCDC) via www.ccdc.cam.ac.uk/data_request/cif

Empirical formula	$C_{21}H_{21}NO_5$	$C_{21}H_{21}NO_5$	$C_{21}H_{21}NO_5$
Formula weight	367.39	367.39	367.39
Temperature	289(2)	313(2)	343(2)
Wavelength (Å)	0.71073	0.71073	0.71073
R_{int} (all data)	0.0549	0.0730	0.0821
Crystal system	triclinic	triclinic	triclinic
Space group	P_{-1}	P_{-1}	P_{-1}
Unit cell dimensions	a = 7.9414(6), α = 71.148°(3) b = 9.2292(7), β = 82.961°(3) c = 13.4539(11), γ = 81.232°(3)	a = 7.9467(3), α = 71.2010° (10) b = 9.2458(4), β = 83.031°(2) c = 13.4593(5), γ = 81.265°(2)	a = 7.9609(7), α = 71.232°(3) b = 9.2958(7), β = 83.063°(3) c = 13.4749(11), γ = 81.143°(3)
Volume ($Å^3$)	919.44(13)	922.52(6)	930.19(12)

Z	2	2	2
Density	1.327	1.323	1.297
Absorption coefficient	0.095	0.095	0.092
F (000)	388	388	380
Crystal size	0.210 X 0.140 X 0.098	0.450 X 0.420X 0.410	0.56X 0.540X 0.450
Theta max	26.393	30.311	30.283
Theta min	2.398	2.344	2.332
Reflections collected	34555	5444	5182
Independent reflections	2553	2532	1872
Absorption correction	SHELXL-2018/3 (Sheldrick, 2018)	SHELXL-2018/3 (Sheldrick, 2018)	SHELXL-2018/3 (Sheldrick, 2018)
Max. and min. Transmission	0.9705 and 0.9158	0.962 and 0.959	0.963 and 0.960
Goodness-of-fit on F ^{2}	1.175	1.059	1.310
R1	0.0518	0.0747	0.2792
wR2	0.1603	0.2045	0.4978

Table S2 GC-MS method applied for all the monomers.

Ramp	Initial oven temp (°C)	Final oven temp (°C)	Heating rate (°C/min)	Hold time (min)	Total run time (min)
I	50	50	0	1	1
II	50	150	10	5	16
III	150	300	10	0	31

Table S3 Parameters from DSC thermograms of monomers recorded at various heating rates.

Heating rate (^{o}C min^{-1})	T_p (°C)		
	oV-fa-[2]ph	oV-fa-[2]ov	oV-fa-[2]v
5	200	178	167
7.5	208	181	172
10	214	187	181
15	215	193	190
20	226	199	197

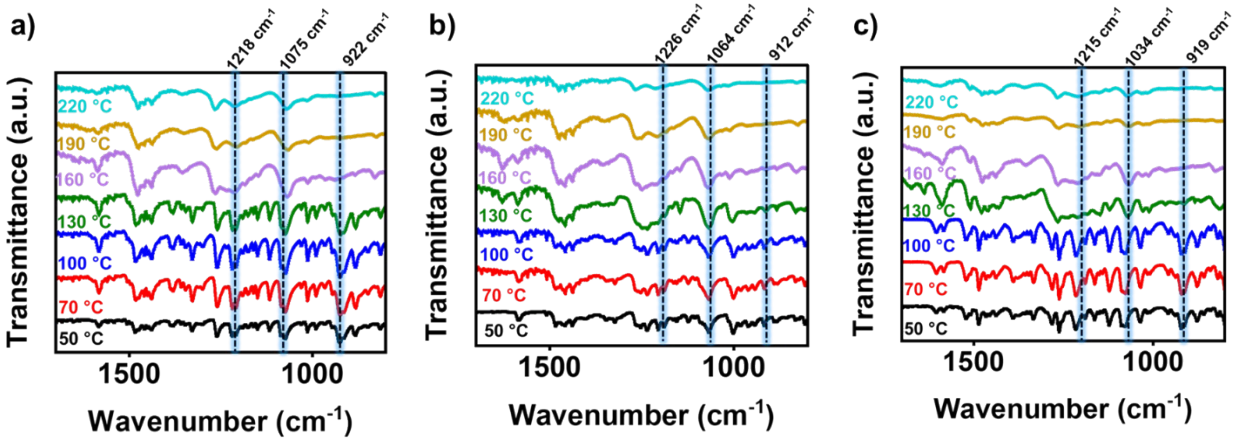

Fig. S9 Stacked FTIR spectra of non-isothermally polymerized monomers. (a) oV-*fa*-[2]ph, (b) oV-*fa*-[2]ov, and (c) oV-*fa*-[2]v.

Synthesis of cardanol based benzoxazine monomer (C-a)[1]

To a stirring mixture of cardanol (5.00 g, 16.61 mol), paraformaldehyde (1.00 g, 33.22 mmol), aniline (1.51 mL, 16.61 mol) was gradually added before heating it slowly from room temperature to 80 ^{o}C and then at 90 ^{o}C for 1 and 2 h, respectively. Thereafter water (10 mL) was added, and the organic layer was extracted with ethyl acetate (3 × 20 mL). The combined organic layers were washed with aqueous sodium hydroxide (0.5 N, 100 mL) before the addition of sodium sulfate. After filtering, solvent was reduced *in vacuo* to yiled C-a as a red oil (92%); FTIR-ATR (diamond crystal/cm^{-1}) 3008, 2926, 2852,1620, 1595, 1573, 1365, 1257, 1224, 1111, 1036, 990, and 960; ^{1}H NMR (400 MHz, $CDCl_3$, ppm): 1.01 (CH_3,t), 1.41 [$(CH_2)_n$, m], 1.67, 2.13 (CH_2CH=, m), 2.49 (CH_2Ar, t), 2.92 [$CH_2(CH=)_2$, m], 4.67 (s, $ArCH_2N$-), 5.41 (-CH=CH=, dd), 5.30-5.41 (m, CH=, CH_2=CH-, -OCH_2N-, -$HC=CH_2$), 6.75(ArH, s), 6.82(ArH, d), 7.00 (ArH, m), 7.20 (ArH, d), 7.34 (ArH, m); ^{13}C NMR (100 MHz, $CDCl_3$, ppm): 50.45 ($ArCH_2N$), 79.45 (-OCH_2N-).

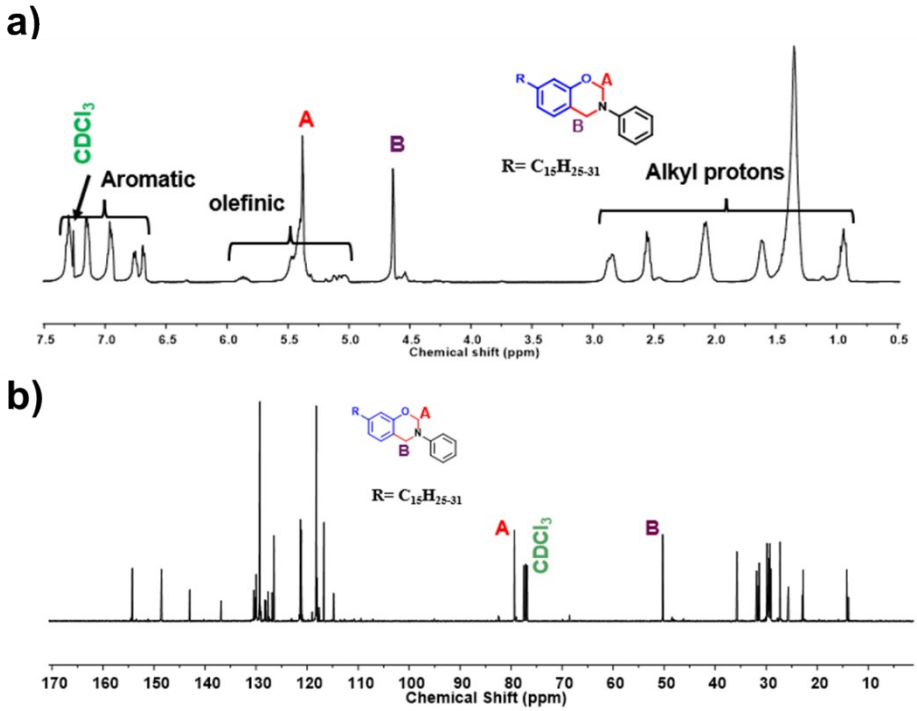

Fig. S10 NMR spectra of C-a monomer: (a) ^{1}H and (b) ^{13}C.

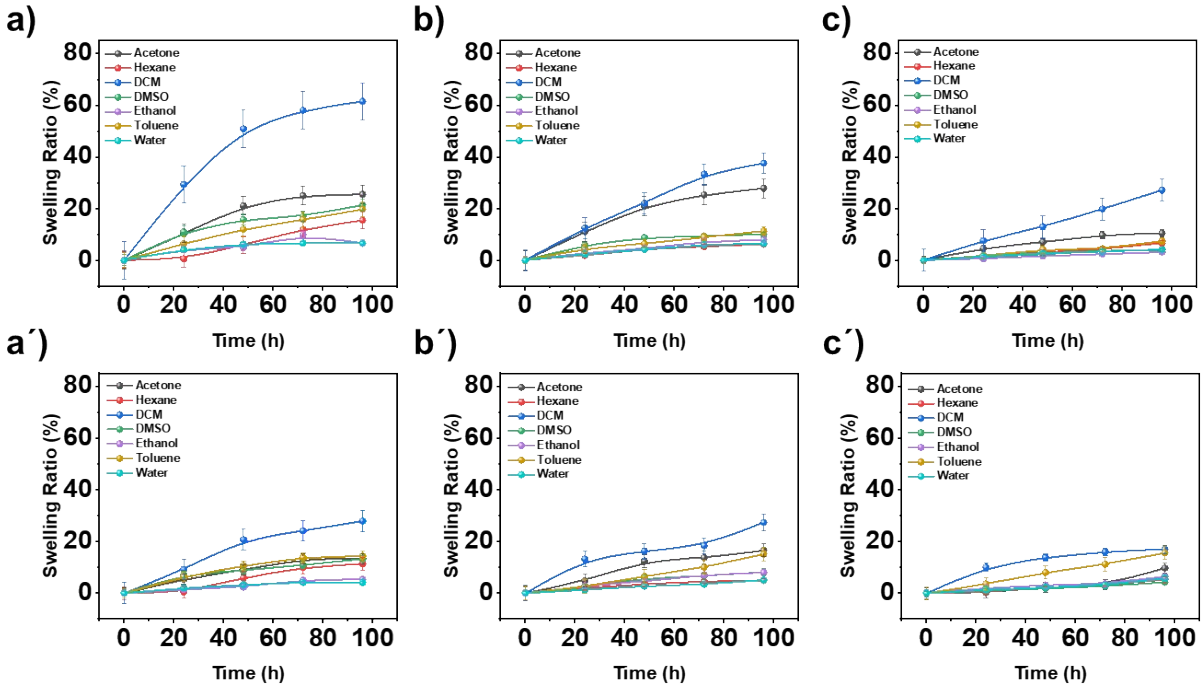

Fig. S11. Variation in swelling ratio with time for (a) poly(oV-fa-[2]ph), (b) poly(oV-fa-[2]ov), (c) poly(oV-fa-[2]v), (a′) poly(Op_1Ca_1), (b′) poly(Oo_1Ca_3) and (c′) poly(Ov_1Ca_3) .

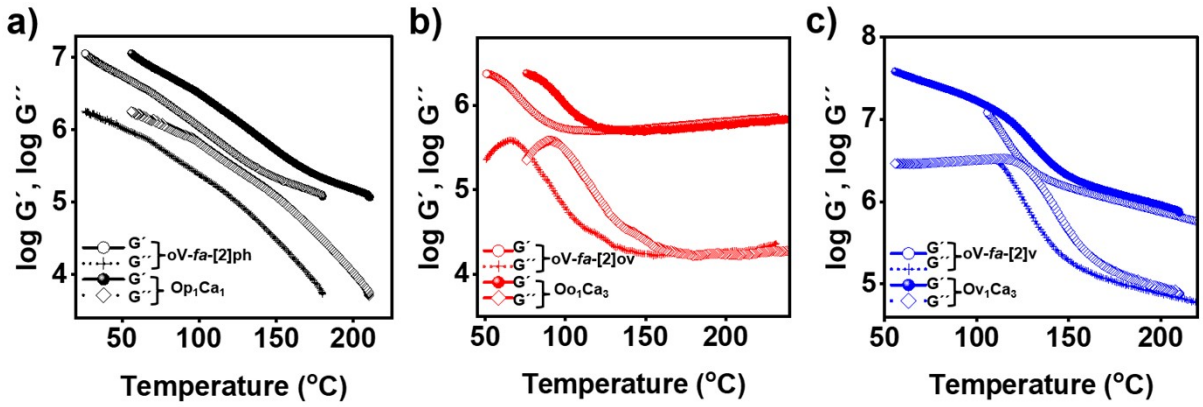

Fig. S12 Storage modulus (log G′) and loss modulus (log G′′) plots of homo and copolymers: (a) poly(oV-*fa*-[2]ph) and its copolymer, (b) poly(oV-*fa*-[2]ov) and its copolymer, and (c) poly(oV-*fa*-[2]v) and its copolymer.

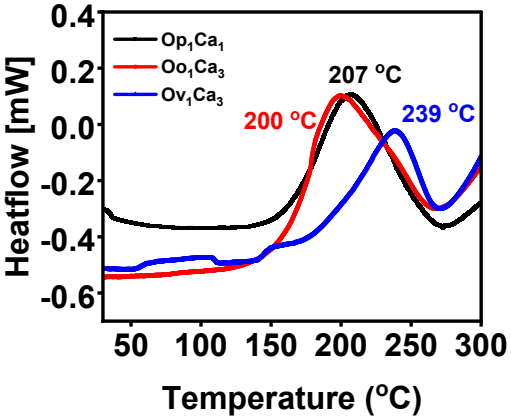

Fig. S13 DSC thermograms of the monomer blends. Heating rate of 10 °C min^{-1} under N_2 atmosphere.

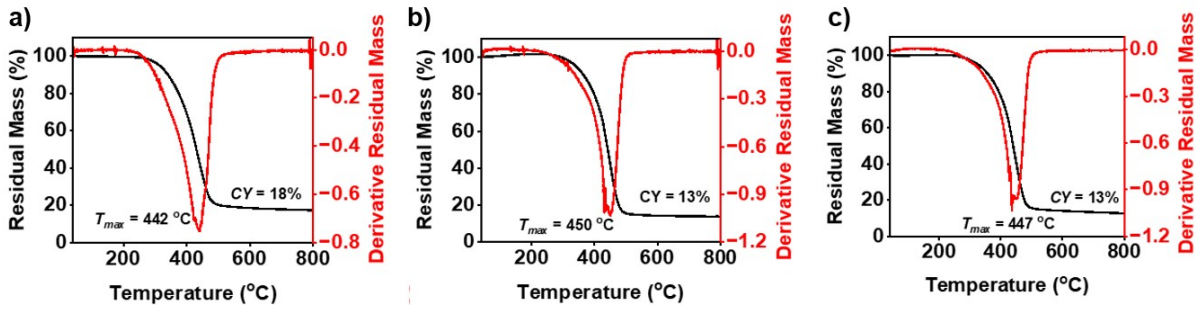

Fig. S14 TGA and DTG plots for the copolymers (a) poly(oV-*fa*-[2]ph), (b) poly(oV-*fa*-[2]ov), (c) poly(oV-*fa*-[2]v), at a heating rate of 10 °C min^{-1}, under an inert N_2 atmosphere.

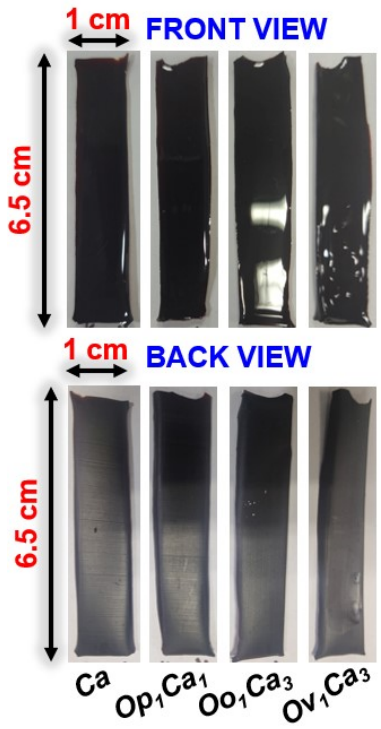

Fig. S15 Representative digital images of the samples for mechanical properties [l × w × h: (65 ± 0.1) mm × (10 ± 0.1) mm × 5 mm].

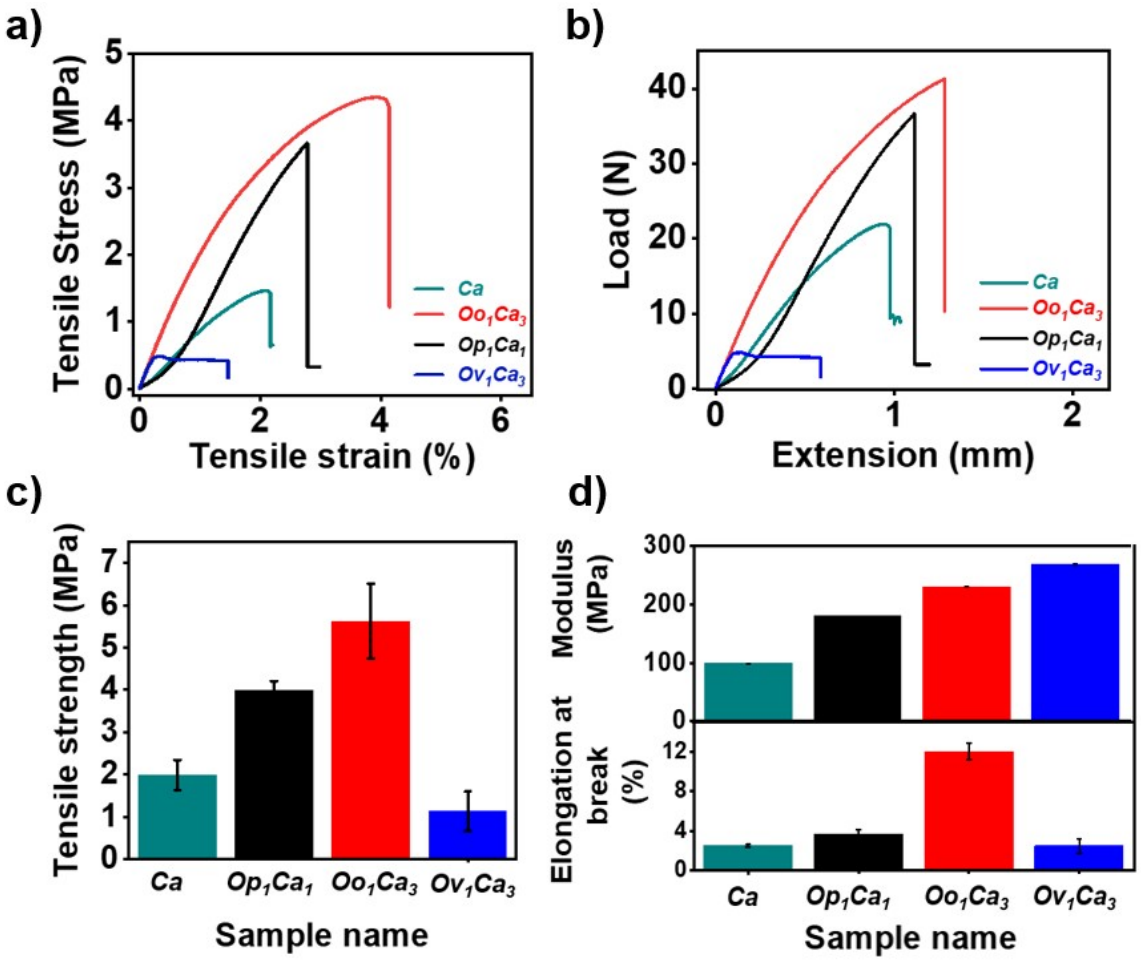

Fig. S16 Mechanical properties of bare polybenzoxazine thermoset of cardanol-aniline and its blend with 4th generation benzoxazines. Curves for (a) tensile stress *vs* tensile strain, and (b) load *vs* extension of different samples. Variation in (c) tensile strength, (d) modulus (above) and elongation at break (below).

References

1. S. Shukla, A. Mahata, B. Pathak and B. Lochab, *RSC Adv.*, 2015, **5**, 78071-78080.